A numerical study of the nonlinear cascade of energy in magnetohydrodynamic turbulence

M. K. Verma

Department of Physics, Indian Institute of Technology, Kanpur

D. A. Roberts, M. L. Goldstein, S. Ghosh, and W. T. Stribling

NASA Goddard Space Flight Center, Greenbelt, Maryland

Abstract. Power spectra of solar wind magnetic field and velocity fluctuations more closely resemble those of turbulent fluids (spectral index of $-5/3$) than they do predictions for magnetofluid turbulence (a $-3/2$ index). Furthermore, the amount the solar wind is heated by turbulence is uncertain. To aid in the study of both of these issues, we report numerically derived energy cascade rates in magnetohydrodynamic (MHD) turbulence and compare them with predictions of MHD turbulence phenomenologies. Either of the commonly predicted spectral indices of 5/3 and 3/2 are consistent with the simulations. Explicit calculation of inertial range energy cascade rates in the simulations show that for unequal levels of fluctuations propagating parallel and antiparallel to the magnetic field, the majority species always cascades faster than does the minority species, and the cascade rates are in better agreement with a Kolmogoroff-like MHD turbulence phenomenology than with a generalized Kraichnan phenomenology even in situations where the fluctuations are much smaller than the mean magnetic field. The "Kolmogoroff constant" for MHD turbulence for small normalized cross helicity is roughly 6.7 in two dimensions and 3.6 for one calculation in three dimensions. For large normalized cross helicity, however, none of the existing models can account for the numerical results, although the Kolmogoroff-like case still works somewhat better than the Kraichnan-like. In particular, the applied magnetic field has much less influence than expected, and Alfvénicity is more important than predicted. These results imply the need for better phenomenological models to make clear predictions about the solar wind.

Introduction

Hot high-speed solar wind streams tend to contain highly Alfvénic fluctuations (i.e., the magnetic and velocity fluctuations are nearly equipartitioned in energy and are highly correlated in direction) and are heated as they move outward in the heliosphere (see *Tu and Marsch* [1995] and *Goldstein et al.* [1995] for recent reviews). The Alfvénic character of most flows vanishes at large distances from the Sun, and in the process the power spectrum of the magnetic and velocity fields becomes Kolmogoroff-like with a $-5/3$ spectral index [*Matthaeus and Goldstein*, 1982; *Tu et al.*, 1990]. This slope is contrary to the expectation of *Iroshnikov* [1964] and *Kraichnan* [1965], who predicted $-3/2$ for the spectral index of magnetohydrodynamic (MHD) turbulence. These characteristics of the spectral evolution, heating,

and spectral indices of the solar wind then lead naturally to the question of the proper theoretical treatment of MHD turbulence and its dissipation.

We will be working in the framework of the standard MHD equations. Throughout the paper, in place of **u** and **B**, we use Elsässer variables [*Elsässer*, 1950, 1956] $\mathbf{z}^{\pm}$, defined as $\mathbf{u} \pm \mathbf{B}$, with $\mathbf{B} \equiv \mathbf{B}'/\sqrt{4\pi\rho}$ where **u** and **B'** are velocity and magnetic field, and ρ is the density. The fluctuations $\mathbf{z}^{\pm}$ represent the Alfvén "waves" traveling "antiparallel" and "parallel" to the mean magnetic field respectively. (The quotes indicate that the waves are not traveling strictly antiparallel and parallel, but have positive and negative correlations between their velocity and magnetic field fluctuations.) These waves couple nonlinearly. Elsässer variables are useful for describing incompressible MHD because in the ideal, nonexpanding limit, either $\mathbf{z}^{+}$ or $\mathbf{z}^{-} = 0$ is an exact solution. The dissipationless momentum and induction equations in the original variables are

$$\frac{\partial \mathbf{u}}{\partial t} + \mathbf{u} \cdot \nabla \mathbf{u} = \mathbf{B} \cdot \nabla \mathbf{B} - \frac{1}{\rho}\nabla p \qquad (1)$$

$$\frac{\partial \mathbf{B}}{\partial t} + \mathbf{u} \cdot \nabla \mathbf{B} = \mathbf{B} \cdot \nabla \mathbf{u} \qquad (2)$$

where p is the thermal pressure. When written in terms of the Elsässer variables, these become

$$\frac{\partial \mathbf{z}^{\pm}}{\partial t} = -\mathbf{z}^{\mp} \cdot \nabla \mathbf{z}^{\pm} \pm \mathbf{B}_0 \cdot \nabla \mathbf{z}^{\pm} - \frac{1}{\rho}\nabla p \qquad (3)$$

where $\mathbf{B}_0$ is the mean magnetic field. Note that if either $\mathbf{z}^+$ or $\mathbf{z}^-$ is zero, there are no nonlinear interactions. The nonlinear terms serve to couple different scales or wave vectors. We assume incompressibility with $\rho = $ const and $\nabla \cdot \mathbf{z}^{\pm} = \mathbf{0}$.

In fluid turbulence there is a conservative transport of energy in wavenumber space that is only stopped by the formation and dissipation of very small structures. The Elsässer variables are convenient for the study of MHD cascades because the energies associated with them, $E^{\pm} = \int (z^{\pm})^2 d^3\mathbf{x}$, are individually conserved and thus we can track their paths through Fourier space. The Reynolds number $R_e = UL/\nu$ measures the relative strength of the nonlinear and viscous stresses at the correlation scale L of the fluctuations with typical speed U in a fluid with kinematic viscosity ν; as R_e increases, the scale for dissipation decreases such that the rate of energy cascade through the inertial range Π is on average equal to the small-scale dissipation rate ϵ in steady state. (The "inertial range" consists of those scales much smaller than the largest "energy containing" eddies, but much larger than the scale where dissipation is important compared to inertial nonlinear terms.) The cascade rate is thought to be independent of R_e, and this assumption yields the Kolmogoroff spectrum for statistically steady, isotropic fluid turbulence. In particular, assuming that the cascade rate only depends on the energy per wavenumber, E_k, and the scalar wavenumber $k = |\mathbf{k}|$ for an isotropic shell in the k-space, then the characteristic nonlinear "eddy turnover time" for fluctuations with velocity amplitude $v_k = (kE_k)^{1/2}$ is $\tau_{NL} = 1/(kv_k)$, and thus the cascade rate can be found from

$$\Pi_{Ko} = \epsilon_{Ko} \propto \frac{kE_k}{\tau_{NL}} = k^{5/2}E_k^{3/2} \qquad (4)$$

or

$$E_k = C_K \Pi_{Ko}^{2/3} k^{-5/3} \qquad (5)$$

where C_K is a universal "Kolmogoroff constant." The large, energy-containing scales may either be stirred at a rate that determines the level of the fluctuations by equating the inertial range flux to the energy input rate, or they may be freely decaying. In the latter case, a quasi-equilibrium can be set up with the input into the inertial range given by, for example, the rate of the decay of the large-scale eddies, U^3/L [see Batchelor, 1970; Hollweg, 1986]. A quasi-equilibrium theory for the decay of the large eddies in MHD has recently been developed by Hossain et al. [1995].

The situation for a magnetized plasma is more complex than the fluid case, with both B_0 and the cross helicity $(H_c = (1/4)[(E^+)^2 - (E^-)^2] = (1/2)\int \mathbf{v} \cdot \mathbf{B}d^3\mathbf{x})$ having possible strong effects on the cascade rate [Iroshnikov, 1964; Kraichnan, 1965; Dobrowolny et al., 1980a, b; Grappin et al., 1982, 1983; Matthaeus and Zhou, 1989; Zhou and Matthaeus, 1990; Tu and Marsch, 1990]. The strength of the background magnetic field controls the propagation of the waves and may also produce spectral anisotropies, which we ignore here, although they must be considered in a more general treatment [see Shebalin et al., 1983; Carbone and Veltri, 1990; Oughton et al., 1994; Hossain et al., 1995]. Strong fields should decrease the interaction time of the eddies [Kraichnan, 1965], as can be seen as follows: If τ_{NL} is the time for the nonlinear term to change the velocity substantially in the absence of magnetic fields (as above), and if one assumes that the field is strong, then Alfvénic propagation limits the interaction time to $\tau_A = 1/(kV_A)$ where V_A is the Alfvén speed, equal to the applied field B_0 in our units. It would take τ_{NL}/τ_A coherent interactions each of time τ_A to produce the same change as τ_{NL} without the field, but if we suppose that each interaction is independent of the others, it will take $(\tau_{NL}/\tau_A)^2$ interactions (N^2 steps to move by N in a random walk). This means the time for spectral transfer will be increased from τ_{NL} to $\tau_s \equiv (\tau_A)(\tau_{NL}/\tau_A)^2 = \tau_{NL}(\tau_{NL}/\tau_A)$ so that the cascade rates will become smaller by τ_A/τ_{NL}. Thus, for the standard Kraichnan phenomenology,

$$\Pi_{Kr} \propto \frac{\tau_A}{\tau_{NL}}\Pi_{Ko} = (1/V_A)k^3 E_k^2 \qquad (6)$$

or

$$E_k = A V_A^{1/2} \Pi_{Kr}^{1/2} k^{-3/2} \qquad (7)$$

where A is the "Kraichnan constant." This equation predicts that a magnetofluid with a strong mean field, such as the solar wind, will have a $-3/2$ spectral index, contrary to solar wind observations (see above). Note that the first part of (6) determines the relationship between the fluxes in a self-similar inertial range for a given wavenumber and power level; the actual spectral levels will be determined for real cases by the energy input at large scales [Hossain et al., 1995; Matthaeus and Zhou, 1989] or by a relaxation from initial conditions [Tu et al., 1984; Tu, 1988].

The nonlinear times for the Elsässer variables are $\tau_{NL}^{\pm} = 1/(k^3 E^{\mp})^{1/2}$ because, according to (3), it is z^+ that convects z^- and visa versa. This gives, for small B_0 and thus large τ_A,

$$\Pi_{Ko}^{\pm} \propto \frac{kE_k^{\pm}}{\tau_{NL}^{\pm}} = k^{5/2}E_k^{\pm}(E_k^{\mp})^{1/2} \qquad (8)$$

Assuming, for simplicity (and in accord with observations for well-developed spectra [e.g., Tu et al., 1990], as well as the simulations below), that the spectra $E_k^{\pm}$ have the same power law, this becomes

$$E_k^\pm = C^\pm (\Pi_{Ko}^\pm)^{4/3} (\Pi_{Ko}^\mp)^{-2/3} k^{-5/3}, \qquad (9)$$

For small normalized cross helicity $\sigma_c = (E^+ - E^-)/(E^+ + E^-)$ we expect $C^+ \approx C^-$, and as a test of the simplest case, we will make predictions with this always the case.

When the Alfvénic decorrelation time is small, by the same reasoning as above,

$$\Pi_{Kr}^\pm = \frac{\tau_A}{\tau_{NL}^\pm} \Pi_{Ko} = A^{-2}(1/V_A)k^3 E_k^+ E_k^- \qquad (10)$$

which, under the assumption of the same power laws for the two species of fluctuations, gives the same spectral equation as before because the cascade rates of $z^\pm$ are always the same as each other. (We ignore the possibility of differing $A^\pm$, as with $C^\pm$.) By contrast, from (9) we find (with $C^+ = C^-$)

$$\frac{E^-(k)}{E^+(k)} = \left(\frac{\Pi^-}{\Pi^+}\right)^2. \qquad (11)$$

which implies unequal cascade rates whenever the spectra of $z^\pm$ differ in amplitude. We will also use this equation to test whether the predictions of the Kolmogoroff-like model agree with simulation results. *Dobrowolny et al.* [1980a, b] were the first to make the arguments for cascade rates involving cross helicity, and they used (10) for cascade rates to argue that solar wind fluctuations will have increasing cross helicity if they are predominantly of one sign initially ("dynamic alignment"). This does not occur in the solar wind due to the small cross helicity at large scales [*Roberts et al.*, 1987, 1992].

Matthaeus and Zhou [1989] and *Zhou and Matthaeus* [1990] generalized the Kolmogoroff-like and Dobrowolny et al.'s generalized Kraichnan model and obtained

$$\Pi^\pm = \frac{A^{-2} E^+(k) E^-(k) k^3}{C_A + \sqrt{k E^\mp(k)}}. \qquad (12)$$

Matthaeus and Zhou's model leads to Kolmogoroff-like or Kraichnan-like models in the limits mentioned above. We will only consider the limiting cases here; consideration of intermediate cases does not change the basic results. *Grappin et al.* [1982, 1983] generalized Kraichnan's model using Eddy-Damped Quasi Normal Markovian (EDQNM) closure calculations. They found that $m^+ + m^- = 3$ where $E_k^\pm = D^\pm k^{-m^\pm}$. The difference in the two slopes is probably quite small except when the cross helicity and Reynolds numbers are very high. Such cases will be left for future work.

Simulations

A number of researchers have performed numerical simulations and compared the results with the spectral-index predictions from the above mentioned models. *Biskamp and Welter* [1989], using 1024×1024 mode simulations, found spectral indices close to $-3/2$. However, they also observed that the indices are approximately $-5/3$ in states in which turbulence concentrated in regions of weak magnetic field. *Pouquet et al.* [1988] and *Politano et al.* [1989] found that at low normalized cross helicity, it was difficult to discriminate between $k^{-5/3}$ and $k^{-3/2}$ energy spectra; however, as the cross helicity increased, the spectral indices m^+ and m^- of E^+ and E^- became somewhat different but their sum remained close to three.

Since $-5/3$ and $-3/2$ are difficult to distinguish, here we numerically study the energy cascade rates in two and three dimensions and compare them with the predictions of the models. Most of the runs were performed in two dimensions because of the expense associated with large three-dimensional runs. The above phenomenological arguments do not depend on dimensionality, and general arguments predict a forward cascade of total energy in both two and three dimensions [*Matthaeus et al.*, 1984; *Matthaeus and Montgomery*, 1984], so that restricting most of our analysis to two dimensions should not significantly affect our conclusions. However, some quantitative differences are expected in two and three dimensions; for example, the constants $C^\pm$ may depend on dimensionality, and we plan to continue our studies of the three-dimensional case.

We solve the incompressible MHD equations (1) − (3) using a pseudospectral method with introduction of hyperviscosity and hyperrestivity [e.g., *Biskamp and Welter*, 1989]. The viscous and resistive terms added to the momentum and induction equations are

$$\nu \left(\nabla^2 \mathbf{u} + \frac{1}{k_{eq}^2} \nabla^4 \mathbf{u}\right) \qquad (13)$$

$$\lambda \left(\nabla^2 \mathbf{B} + \frac{1}{k_{eq}^2} \nabla^4 \mathbf{B}\right) \qquad (14)$$

The viscous and resistive terms thus have a higher order wavenumber dependence; the hyperviscous term $\nu(k^4/k_{eq}^2)u$ becomes dominant only at large wavenumbers ($k \gg k_{eq}$) and forces the energy spectra to become small at these wavenumbers. This minimizes aliasing and ensures the development of a clearly discernible inertial range. In two dimensions we choose $\nu = 5.0\times10^{-6}$ and $k_{eq} = 10.0$ which yields Reynolds numbers (given simply by the inverse of the multiplier of k^2 in the dissipation term in wavenumber space) of approximately 2×10^5 at large scales and 500 at small scales. In three dimensions $\nu = 5.0 \times 10^{-6}$, but $k_{eq} = 2.0$, which implies that the Reynolds number at the largest scales is about 2×10^5, but at small scales it decreases to 200. Note that, as shown below, the dissipation scales are nonetheless resolved and the dissipation term is dominant at high k; this discrepancy is due to the misleading nature of a freqeuntly used definition of the Reynolds number (see the discussion of this point by *Ghosh, et al.* [1996]). The maximum resolution of our simulation in 2-D is 512^2, whereas in 3-D it is 128^3. The runs we consider have $(B_0, \sigma_c) = (0, 0), (0, 0.25), (0, 0.9), (1, 0), (1,$

Table 1. Comparison of $\Pi^{\pm}$ From the Simulations With the Predictions From the Turbulence Phenomenologies.

Run		Π_{sim}		Π_{Ko}/Π_{sim}*		Π_{Kr}/Π_{sim}*		$\dfrac{(E^-/E^+)}{(\Pi^-/\Pi^+)^2}$
B_0	σ_c	+	−	+	−	+	−	
0	0.00	0.015	0.020	0.82	0.79	1.00	0.75	1.0
1	0.00	0.028	0.032	1.11	1.12	2.23	1.95	1.0
0	0.25	0.015	0.010	0.90	0.90	0.50	0.75	1.0
1	0.25	0.040	0.030	1.33	1.26	1.75	2.33	0.9
5	0.25	0.060	0.040	0.85	1.1	0.11	0.16	1.7
0	0.90	0.028	0.002	0.50	1.74	0.19	2.39	11
1	0.90	0.033	0.004	0.66	1.57	0.42	3.50	5.9
5	0.90	0.045	0.015	1.00	0.93	0.04	0.11	0.9
0	0.25^{3D}	0.021	0.006	0.94	1.09	0.19	0.66	1.4

* For the Kolmogoroff-like model, the constant $C = 6.7$ for 2-D and 3.6 for 3-D. For the generalized Kraichnan model $A = 2.0$.

0.25), (1, 0.9), (5, 0.25), (5, 0.9) in the two-dimensional runs, and (0, 0.25) in three dimensions. (The σ_c values are for $T = 0$.) In two dimensions the mean magnetic field is in the plane of fluctuations.

The simulations were initialized with a block spectrum out to $k = 4$ in two dimensions for $B_0 = 0.0$ and 1.0, and a k^{-1} spectrum out to $k = 15$ in the three-dimensional run and in two dimensions for $B_0 = 5.0$. In these units, the initial magnetic and velocity fluctuations have root-mean-square amplitudes of unity, and thus $B_0 = 1$ implies equipartition between mean field and fluctuating energy. The initial σ_c is shown in Ta-

ble 1. The kinetic and (fluctuating) magnetic energy are chosen to be equal at $t = 0$. We find that after approximately 10 eddy turnover times (defined in terms of the initial velocity perturbation) the system reaches a fully developed turbulent state, i.e., the energy spectra $E^{\pm}(k)$ exhibit approximate power laws (see Figure 1) with approximately constant inertial range fluxes across a portion of the spectrum (Figure 2). We obtained the spectral indices by fitting a straight line in the inertial range, which we take to be where the spectrum is a
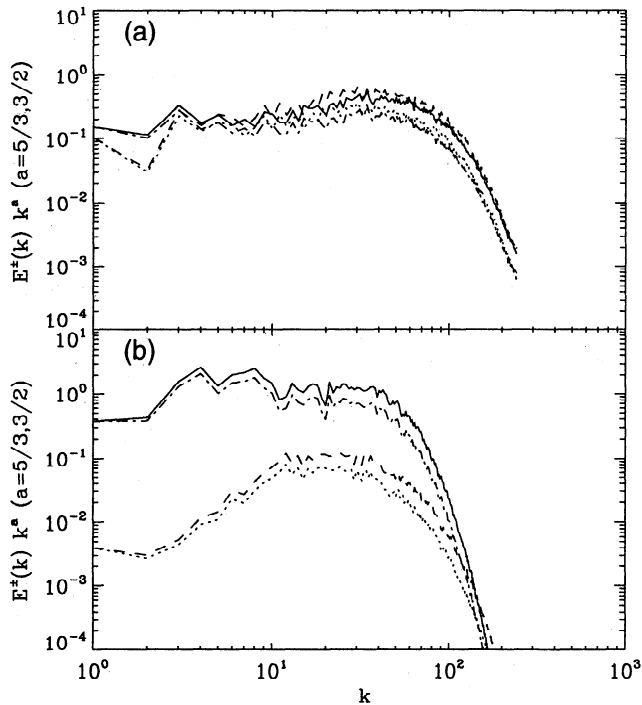

Figure 1. (a) $E^{\pm}(k)k^a$ versus k for a 2-D run with $B_0 = 0.0$ and $\sigma_c = 0.0$, and, (b), $B_0 = 1.0$ and $\sigma_c = 0.9$. The solid (E^+) and dashed (E^-) correspond to $a = 5/3$, and chained (E^+) and dotted (E^-) correspond to $a = 3/2$.
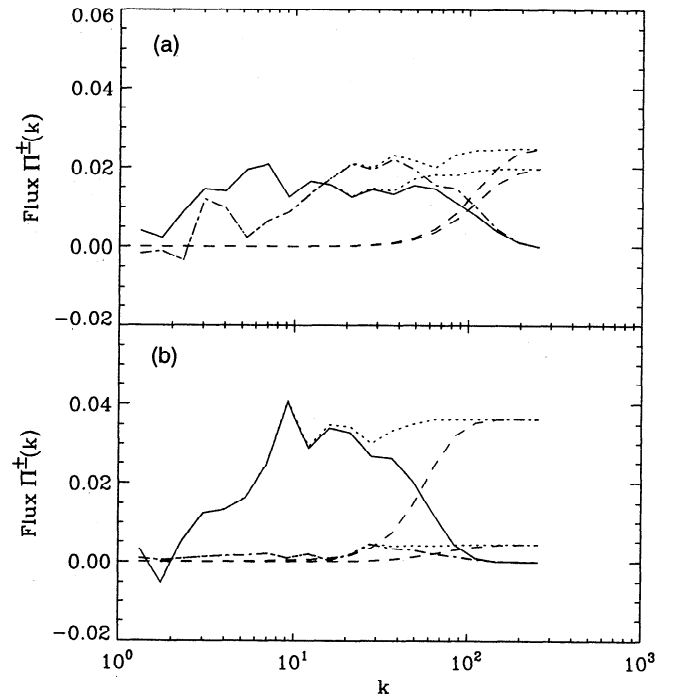

Figure 2. (a) Cascade rates $\Pi^{\pm}(k)$ versus k (solid for plus and chained for minus) for a two-dimensional run with $B_0 = 0.0$ and $\sigma_c = 0.0$, and (b), the same quantities plotted for a run with $B_0 = 1.0$ and $\sigma_c = 0.9$. The dashed lines are viscous dissipation rate, and the dotted lines are the rate of energy loss in a sphere of radius K in Fourier space given by $-(\partial/\partial t)\int_0^K E^{\pm}(k,t)dk$.

power law and the flux is nearly constant, and found that it was difficult to distinguish between the spectral indices of $-3/2$ and $-5/3$. To calculate the energy flux $\Pi^\pm$ leaving a sphere of radius K in wavenumber space from the simulation, we used

$$\Pi^\pm(K) = -\frac{\partial}{\partial t} \int_0^K E^\pm(k, t)dk - 2 \int_0^K \nu_k k^2 E^\pm(k, t)dk,$$

(15)

where $\nu_k = \nu_0[1 + (k/k_{eq})^2]$. The first term in the right hand side is the rate of energy loss in the sphere, whereas the second term is the negative of the viscous dissipation rate in the sphere; the flux flowing out of the sphere to neighboring wavenumbers is the sum of these. In Figure 2 we show the flux $\Pi^\pm$ versus k along with the other two terms in the above equation. That the energy fluxes are very approximately constant in the intermediate range of k and are equal to the overall dissipation rates shows that the simulations are consistent with these phenomenologically assumed properties and indicate a quasi-steady state cascade. Because there is no forcing, this situation is not a true cascade, but it does reflect the situation in the solar wind. However, note that because of the low resolution and the inherent randomness of the flow, the relative fluctuation in the inertial range flux determined by averages at neighboring time steps is as much as 25%, hence the error in results is approximately 25%. The values used for the simulation quantities in Table 1 were found from taking averages in time and wave number for the wavenumbers where fluxes and slopes were judged to be sufficiently constant. No detailed fitting procedure was used since there were no obvious simple criteria for achieving this. As will be seen, the errors involved in this procedure have no effect on the conclusions of this study.

We now compare the predictions of energy fluxes by MHD turbulence phenomenologies with the simulation results computed at times corresponding to Figures 1 and 2 ($T \approx 10 - 13$). Table 1 contains energy fluxes, the ratios of predicted (Π_{Ko} and Π_{Kr}) to simulated (Π_{sim}) energy fluxes with cascade constants chosen to give good agreement at low σ_c, and the ratio $(E_k^-/E_k^+)/(\Pi^-/\Pi^+)^2$ from the simulations. In our simulations the mean magnetic field (or the magnetic field of the largest eddies for the Kraichnan-like case with $B_0 = 0$) were at least ≈ 1, whereas the amplitudes of the largest $z^\pm$ fluctuations in the inertial range ($k > 10$) were 0.2 to 0.5 (the initial fluctuating magnetic and kinetic energy were 0.5 in dimensionless units). Hence $z^\pm < C_A$, and according to the assumptions of the phenomenological models, we expect the generalized Kraichnan model to be applicable with $\Pi^+ \approx \Pi^-$. However, the simulation results show that the flux of the majority species (greater of E^+ and E^-) is always greater than that of the minority species (see Table 1). Therefore the predictions of the Kraichnan-like model are inconsistent with the numerical simulations even for $C_A \sim 10z^\pm$ ($B_0 = 5$ in Table 1).

The Kolmogoroff-like phenomenology predicts that (see (11)), $(E_k^-/E_k^+)/(\Pi^-/\Pi^+)^2 = 1$. Our numerical results (see Table 1) are consistent with this prediction for low cross helicity. However, for large σ_c the equality does not hold in the simulations, indicating an inconsistency with the Kolmogoroff-like phenomenology when σ_c is large, although this model's predictions for $\Pi^\pm$ are generally within a factor or two of the simulations. Overall, our results indicate that for large σ_c none of the phenomenologies work well. For relatively large average magnetic fields ($B_0 = 5.0$), the Kolmogoroff-like phenomenology appears to be closer to the truth, even for large σ_c. This is surprising because the larger the average magnetic field, the more accurate Kraichnan's model should be. At present, it is not clear at what value of $V_A/z^\pm$ Kraichnan's model might become applicable, if any (but see the discussion by *Matthaeus and Zhou* [1989]). We find that the mean field suppresses the cascade rate much less than predicted, even in two dimensions; perhaps this is due to preferential couplings transverse to the magnetic field [*Shebalin et al.*, 1983; *Carbone and Veltri*, 1990; *Oughton et al.*, 1995; *Hossain et al.*, 1995]. Both models underestimate the cascade rate of the majority species. Correcting this requires more than a change in the cascade constant because the two species behave differently, and thus this implies that the "constants" must depend on both the species and the net σ_c. For the relatively low resolution three-dimensional simulation with $\sigma_c = 0.25$, we found that the Kolmogoroff-like phenomenology worked well with $C_K = 3.6$.

For completeness, we note that the fluctuating energy decays by about 50% in the runs with low cross helicity and by only 20% in those with high cross helicity. The decay is somewhat faster in cases with a small B_0, but this effect is much smaller than the effect of the cross helicity. The magnetic and kinetic enstrophies (the mean of the square of the current and vorticity, respectively) both increase by at least an order of magnitude in all cases, implying the strong development of small-scale structures. The increase in enstrophies is initially quite rapid, and it is followed at late times by a very slow decay such that the final state in the run still has high enstrophies. The value of σ_c remains low for the cases starting with $\sigma_c = 0$, whereas it increases somewhat for the nonzero initial cross-helicity cases. The $\sigma_c = 0.9$ case becomes nearly "dynamically aligned" with σ_c near 1 (e.g., 0.98). The implications of this wil be left for other work.

Conclusions

From our simulations it is not possible to distinguish between spectral indices of $-5/3$ and $-3/2$. The cascade rate studies, however, provide additional insights into MHD turbulence phenomenologies. For small σ_c, the cascade rates of the majority species are greater than those of minority species, and agree better with the

Kolmogoroff-like MHD turbulence phenomenology than with the Kraichnan-like model even when $z^{\pm} \ll C_A$. These results are contrary to the assumptions of the existing phenomenologies, but are in agreement with the solar wind observations which show $k^{-5/3}$ energy spectra although $z^{\pm} < C_A$. (Intermittency may affect the spectral slopes in this case, but it is difficult to believe that the very close agreement with $k^{-5/3}$ found for data sets carefully selected to be stationary [*Matthaeus and Goldstein*, 1982] are the result of a precise change from $k^{-3/2}$ due to intermittency.) The superiority of the Kolmogoroff-like compared to the Kraichnan-like models is also found for the decay of the energy containing scales [*Hossain et al.*, 1995]. From the simulation results we calculate the Kolmogoroff's constant for MHD turbulence and find that for small σ_c it is approximately 6.7 in two dimensions and 3.6 in three dimensions. For large σ_c, however, none of the existing phenomenologies can account for the simulation results, indicating that modifications to the existing models are required.

Recently, *Verma and Bhattacharjee* [1996] have calculated $C^{\pm}$ using the Direct Interaction Approximation (DIA) under the assumption that the energy spectra $E^{\pm}(k)$ follow the Kolmogoroff-like phenomenology. They showed that the constants $C^{\pm}$ are not universal, but depend on the Alfvén ratio (ratio of kinetic and magnetic energy) and the normalized cross helicity. For small σ_c they find that $C \approx 5.4$ in two dimensions and $C \approx 4$ in three dimensions, in fairly good agreement with the values found here. Preliminary DIA calculations with larger σ_c show that $C^- > C^+$ if $E^+(k) > E^-(k)$, similar to what we find in our simulations. The DIA results for large mean fields are not in agreement with the simulations, and the reason for this is not yet known. The difficulty of performing these calculations for a sufficiently broad parameter range has precluded, thus far, a complete calculation of a new phenomenology.

The above considerations apply to quasi-steady state turbulence, whereas, in contrast to these simulations, significant spectral evolution occurs in the solar wind [e.g., *Tu and Marsch*, 1995]. The simplest model for nonsteady cases is to assume that the cascade rate is determined by the steady rate associated with the level of the turbulence in the relevant range in Fourier space and to use this to find the changes in the spectrum with time (see *Goldstein et al.* [1995] for a discussion and references). Simulations with more solar-wind-like initial conditions than those in the present study [*Roberts et al.*, 1991] also show strong spectral evolution. While these ideas have had some success, it remains to be determined if the nonsteady cascades behave in the same way as the steady ones. Simulations to test this are at the outer limits of what is possible on present computers, and we plan to work in this direction. Efforts to study solar wind heating due to turbulent cascades [*Tu*, 1988; *Verma et al.*, 1995] have shown promise, but detailed predictions require refinement of the present de-

velopment. In particular, *Verma et al.* [1995] find that Kolmogoroff-like phenomenology provides a better description of the temperature evolution in the solar wind than does the Kraichnan-like, but that neither is wholly adequate. If the nonsteady cases can be treated successfully by a general phenomenology developed from quasi-steady state simulations, then we will be able to predict with confidence the role of turbulent heating in a wide variety of situations, from solar loops, to the outer heliosphere, to more distant astrophysical objects.

References

Batchelor, G. K., *Theory of Homogeneous Turbulence*, Cambridge Univ. Press, New York, 1970.

Biskamp, D., and H. Welter, Dynamics of decaying two-dimensional magnetohydrodynamic turbulence, *Phys. Fluids B*, *1*, 1964, 1989.

Carbone, V., and P. Veltri, A shell model for anisotropic magnetohydrodynamic turbulence, *Geophys. Astrophys. Fluid Dyn.*, *52*, 153, 1990.

Dobrowolny, M., A. Mangeney, and P. Veltri, Fully developed anisotropic turbulence in interplanetary space, *Phys. Rev. Lett.*, *45*, 144, 1980a.

Dobrowolny, M., A. Mangeney, and P. Veltri, Properties of mhd turbulence in the solar wind, *Astrophys. J.*, *83*, 2632, 1980b.

Elsässer, W. M., The hydromagnetic equations, *Phys. Rev.*, *79*, 183, 1950.

Elsässer, W. M., Hydromagnetic dynamo theory, *Rev. Mod. Phys.*, *18*, 135, 1956.

Ghosh, S., E. Siregar, D. A. Roberts, and M. L. Goldstein, Simulation of high-frequency solar wind power spectra using Hall magnetohydrodynamics, *J. Geophys. Res.*, *101*, 2493, 1996.

Goldstein, M. L., D. A. Roberts, and W. H. Matthaeus, Magnetohydrodynamic turbulence in cosmic winds, in *Cosmic Winds and the Heliosphere*, edited by J. R. Jokipii and C. P. Sonett, Univ. of Ariz. Press, Tucson, in press, 1995.

Grappin, R., U. Frisch, J. Léorat, and A. Pouquet, Alfvénic fluctuations as asymptotic states of MHD turbulence, *Astron. Astrophys.*, *105*, 6, 1982.

Grappin, R., A. Pouquet, and J. Léorat, Dependence of MHD turbulence spectra on the velocity field-magnetic field correlation, *Astron. Astrophys.*, *126*, 51, 1983.

Hollweg, J. V., Transition region, corona, and solar wind in coronal holes, *J. Geophys. Res.*, *91*, 4111, 1986.

Hossain, M., P. C. Gray, D. H. Pontius Jr., W. H. Matthaeus, and S. Oughton, Phenomenology for the decay of energy-containing eddies in homogeneous mhd turbulence, *Phys. Fluids*, *7*, 2886, 1995.

Iroshnikov, P. S., Turbulence of a conducting fluid in a strong magnetic field, *Sov. Astron.*, *7*, 566, 1964.

Kraichnan, R. H., Inertial range of hydromagnetic turbulence, *Phys. Fluids*, *8*, 1385, 1965.

Matthaeus, W. H., and M. L. Goldstein, Measurement of the rugged invariants of magnetohydrodynamic turbulence, *J. Geophys. Res.*, *87*, 6011, 1982.

Matthaeus, W. H., and D. Montgcmery, Dynamic alignment and selective decay in magnetohydrodynamics, in *Statistical Physics and Chaos in Fusion Plasmas*, edited by C. W. Horton and L. E. Reichl, p. 285, John Wiley, New York, 1984.

Matthaeus, W. H., and Y. Zhou, Extended inertial range phenomenology of magnetohydrodynamic turbulence, *Phys. Fluids B, 1*, 1929, 1989.

Matthaeus, W. H., M. L. Goldstein, and D. C. Montgomery, Turbulent generation of outward traveling interplanetary Alfvénic fluctuations, *Phys. Rev. Lett., 51*, 1484, 1984.

Oughton, S., Transport of solar wind fluctuations: A turbulence approach, Ph. D. thesis, Univ. of Del., Newark, 1993.

Oughton, S., E. Priest, and W. H. Matthaeus, The influence of a mean magnetic field on three-dimensional mhd turbulence, *J. Fluid Mech., 280*, 95, 1994.

Politano, H., A. Pouquet, and P. L. Sulem, Inertial ranges and resistive instabilities in two-dimensional magnetohydrodynamic turbulence, *Phys. Fluids B, 1*, 2330, 1989.

Pouquet, A., U. Frisch, and J. Léorat, Strong MHD helical turbulence and the nonlinear dynamo effect, *J. Fluid Mech., 77*, 321, 1976.

Pouquet, A., P. L. Sulem, and M. Meneguzzi, Influence of velocity-magnetic field correlations on decaying magnetohydrodynamic turbulence with neutral X points, *Phys. Fluids, 31*, 2635, 1988.

Roberts, D. A., M. L. Goldstein, L. W. Klein, and W. H. Matthaeus, Origin and evolution of fluctuations in the solar wind: Helios observations and Helios-Voyager comparisons, *J. Geophys. Res., 92*, 12,023, 1987.

Roberts, D. A., S. Ghosh, M. L. Goldstein, and W. H. Matthaeus, MHD simulation of the radial evolution and stream structure of solar wind turbulence, *Phys. Rev. Lett., 67*, 3741, 1991.

Roberts, D. A., M. L. Goldstein, W. H. Matthaeus, and S. Ghosh, Velocity shear generation of solar wind turbulence, *J. Geophys. Res., 97*, 17,115, 1992.

Shebalin, J. V., W. H. Matthaeus, and D. Montgomery, Anisotropy in MHD turbulence due to a mean magnetic field, *J. Plasma Phys., 29*, 525, 1983.

Tu, C.-Y., The damping of interplanetary Alfvénic fluctuations and the heating of the solar wind, *J. Geophys. Res., 93*, 7, 1988.

Tu, C.-Y., and E. Marsch, Transfer equations for spectral densities of inhomogeneous MHD turbulence, *J. Plasma Phys., 44*, 103, 1990.

Tu, C.-Y., and E. Marsch, *MHD Structures, Waves and Turbulence in the Solar Wind: Observations and Theories*, Kluwer Acad., Boston, Mass., 1995.

Tu, C.-Y., Z.-Y. Pu, and F.-S. Wei, The power spectrum of interplanetary Alfvénic fluctuations: Derivation of the governing equation and its solution, *J. Geophys. Res., 89*, 9695, 1984.

Tu, C.-Y., E. Marsch, and H. Rosenbauer, The dependence of MHD turbulence spectra on the inner solar wind stream structure near solar minimum, *Geophys. Res. Lett., 17*, 283, 1990.

Verma, M. K., and J. K. Bhattacharjee, Computation of Kolmogorov's constant in magnetohydrodynamic turbulence, *Euro. Phys. Lett., in press*, 1996.

Verma, M. K., D. A. Roberts, and M. L. Goldstein, Turbulent heating and temperature evolution of the solar wind plasma, *J. Geophys. Res., 100*, 19,839, 1995.

Zhou, Y., and W. H. Matthaeus, Models of inertial range spectra of interplanetary magnetohydrodynamic turbulence, *J. Geophys. Res., 95*, 14881, 1990.

S. Ghosh, M. L. Goldstein, D. A. Roberts, and W. T. Stribling, Laboratory for Extraterrestrial Physics, NASA Goddard Space Flight Center, Greenbelt, MD 20771.

M. K. Verma, Department of Physics, Indian Institute of Technology, Kanpur, 208016, India.